Size-dependent transition to high-symmetry chiral structures in AgCu, AgCo, AgNi and AuNi nanoalloys - Online supporting information

D. Bochicchio and R. Ferrando

Dipartimento di Fisica and CNISM, Via Dodecaneso 33, Genova, I16146, Italy.

The form of the atom-atom potential used in the simulations is derived with the second-moment approximation to the tight-binding model [1, 2]. The binding energy of the system E is writte as:

$$E = \sum_{i}^{N} [E^r(i) + E^a(i)] \tag{1}$$

$E^r(i)$ and $E^a(i)$ represent repulsive and attractive contributions, respectively, and are defined as

$$\begin{aligned} E^r(i) &= \sum_{i \neq j}^{N} A(a,b) e^{-p(a,b)(r_{ij}/r_0(a,b)-1)} \\ E^a(i) &= \left[\sum_{i \neq j}^{N} \xi^2(a,b) e^{-2q(a,b)(r_{ij}/r_0(a,b)-1)} \right]^{1/2} \end{aligned} \tag{2}$$

where *a*(*b*) represent the atomic species of atom *i* (*j*), r_{ij} is the distance between these atoms, and r_0, ξ, q, p and A are adjustable parameters. For a binary system a set of 15 parameters (5 for each element plus 5 describing the mixing) need to be defined, of which only 12 are independent (it is always possible to adjust the other parameters to changes in r_0). Here we present two parameter sets, named P1 and P2. The results in the Letter are obtained by P1, unless otherwise specified. Parameter sets for both potentials are reported in Table I. P2 was used in Refs. [3–5]. P1 has been refitted in order to achieve a better agreement with Density-Functional results for surface energies and the energetics of small clusters (up to 55 atoms, see Tables II and III), while reproducing the experimental data for lattice spacing, cohesive energy and bulk modulus for the pure elements. The results of both potentials are compared to the DF results for larger clusters (size between 100 and 300 atoms) in Table IV.

As follows from the analysis of the results, the agreement between DF calculations and P1 results is very good in the whole nanoalloy size range. P1 and DF always agree for the lowest energy structure. The agreement improves with increasing size. In fact, for sizes above 100 atoms, the energetic ordering of the isomers is always correctly reproduced, with a good quantitative agreement for the energy differences. For small sizes, some discrepancies remains, that we were not able to overcome by means of this simple interaction model. The agreement between P2 and DF is also good, even though P2 is not able to single out the lowest-energy structures of $Ag_{32}Cu_6$ and $Ag_{132}Cu_{147}$. In the latter case, energies of anti-Mackay and chiral icosahedra are however quasi-degenerate. The quantitative agreement of P2 with DF for the energy differences between isomers is on average somewhat worse than for the P1. We remark however that overall trends are the same for all calculations.

[1] F. Cyrot-Lackmann and F. Ducastelle, Phys. Rev. B **4**, 2406 (1971).

[2] R. P. Gupta, Phys. Rev. B **23**, 6265 (1985).

[3] F. Baletto, C. Mottet, and R. Ferrando, Phys. Rev. B **66**, 155420 (2002).

[4] F. Baletto, C. Mottet, and R. Ferrando, Phys. Rev. Lett. **90**, 135504 (2003).

[5] G. Rossi, A. Rapallo, C. Mottet, A. Fortunelli, F. Baletto, and R. Ferrando, Phys. Rev. Lett. **93**, 105503 (2004).

[6] F. R. Negreiros, G. Barcaro, Z. Kuntová, G. Rossi, R. Ferrando, and A. Fortunelli, J. Chem. Phys. **132**, 234703 (2010).

[7] P. Giannozzi et al., J. Phys. Cond. Mat. **21**, 395502 (2009).

[8] J. P. Perdew, K. Burke, and M. Ernzerhof, Phys. Rev. Lett. **77**, 3865 (1996).

TABLE I:

	P1			P2		
Parameters	Ag-Ag	Cu-Cu	Ag-Cu	Ag-Ag	Cu-Cu	Ag-Cu
A(eV)	0.0801	0.0834	0.0900	0.1031	0.0894	0.0977
ξ(eV)	1.0883	1.2167	1.1115	1.2799	1.2799	1.2275
p(eV)	12.0	11.0	11.111	10.85	10.55	10.70
q(eV)	2.85	2.30	2.013	3.18	2.43	2.805
r_0(Å)	2.89	2.56	2.725	2.89	2.56	2.725

TABLE II: Surface energies γ (in mJ/m^2) for three low-index facets of pure Ag and Cu fcc bulk systems. For the values of the parameters, see Table I. DF calculations [6] are made by the Quantum Espresso package [7] and use the PBE exchange-correlation functional [8].

Element	Quantity	Density Functional	P1	P2
Ag	γ_{111}	738	710	586
	γ_{100}	788	790	659
	γ_{110}	889	857	724
Cu	γ_{111}	1269	1211	1074
	γ_{100}	1360	1309	1156
	γ_{110}	1507	1412	1290

TABLE III: . Energetics of Mackay and anti-Mackay icosahedra for pure Ag and Cu clusters of size 45. The structures are shown in Fig. 1. Energies are given in eV.

System	Structure	Density Functional	P1	P2
Ag_{45}	Mackay1	0.000	0.000	0.000
Ag_{45}	anti-Mackay	3.060	3.865	4.795
Cu_{45}	Mackay1	0.000	0.000	0.000
Cu_{45}	anti-Mackay	3.523	2.683	2.313

TABLE IV: Energetics of small-size nanoalloys. For each size and composition, the data report the energy difference from the most stable isomer according to DF calculations, which is taken as the zero of the energy. The structures are shown in Fig. 1, with the exception of the 13-atom icosahedra. Energy differences are given in eV.

size and composition	structure	Density Functional	P1	P2
13 Ag_1Cu_{12}	Ihsup	0.000	0.000	0.000
	Ihcen	1.771	2.522	1.608
13 $Ag_{12}Cu_1$	Ihcen	0.000	0.000	0.000
	Ihsup	0.415	0.233	0.706
34 $Ag_{27}Cu_7$	pc5	0.000	0.000	0.000
	pc5def	0.627	0.531	0.448
	asymm	0.999	0.438	0.305
38 $Ag_{32}Cu_6$	pc5mod	0.000	0.000	0.000
	pc6	0.335	0.320	-0.261
	C_s	0.790	0.226	0.189
	truncated octahedron (TO)	1.585	0.614	0.623
45 $Ag_{32}Cu_{13}$	anti-Mackay	0.000	0.000	0.000
	Mackay1	1.300	0.797	1.081
	Mackay2	1.385	0.422	0.853
55 $Ag_{32}Cu_{13}$	Mackay	0.000	0.000	0.000
	D_{5h}	0.873	0.794	0.747
	Ino decahedron	3.010	3.399	2.628
	cuboctahedron	4.063	4.221	3.287

TABLE V: Energetics of large nanoalloys. For each size and composition, the data report the energy difference from the most stable isomer according to DF calculations, which is taken as the zero of the energy. The structures are shown in Fig. 2. Energy differences are given in eV.

size and composition	structure	Density Functional	P1	P2
127 $Ag_{72}Cu_{55}$	anti-Mackay	0.000	0.000	0.000
	tetraIh	0.644	0.744	1.183
	Mackay	2.013	2.604	2.952
	chiral icosahedron	not stable	not stable	not stable
127 $Ag_{75}Cu_{52}$	tetraIh	0.000	0.000	0.000
	anti-Mackay	1.087	0.752	0.087
146 $Ag_{90}Cu_{56}$	pentaIh	0.000	0.000	0.000
	Mackay	1.220	1.120	2.156
	Marks decahedron	9.460	7.300	7.882
147 $Ag_{92}Cu_{55}$	pentaIh	0.000	0.000	0.000
	Mackay	0.352	0.133	1.357
	Ino decahedron	7.831	7.589	3.901
	cuboctahedron	9.850	9.412	8.296
192 $Ag_{107}Cu_{85}$	chiral C_5	0.000	0.000	0.000
	Marks decahedron	7.991	7.412	7.602
279 $Ag_{132}Cu_{147}$	anti-Mackay	0.000	0.000	0.000
	chiral icosahedron	0.430	0.072	-0.132
	Mackay	7.083	7.943	7.467
509 $Ag_{200}Cu_{309}$	chiral icosahedron	—	0.000	0.000
	anti-Mackay	—	1.666	1.718
521 $Ag_{212}Cu_{309}$	chiral icosahedron	—	0.000	0.000
	anti-Mackay	—	not stable	2.171
873 $Ag_{312}Cu_{561}$	chiral icosahedron	—	0.000	0.000
	anti-Mackay	—	not stable	6.448

FIG. 1: Structures of small size nanoalloys. Dh stands for decahedron.

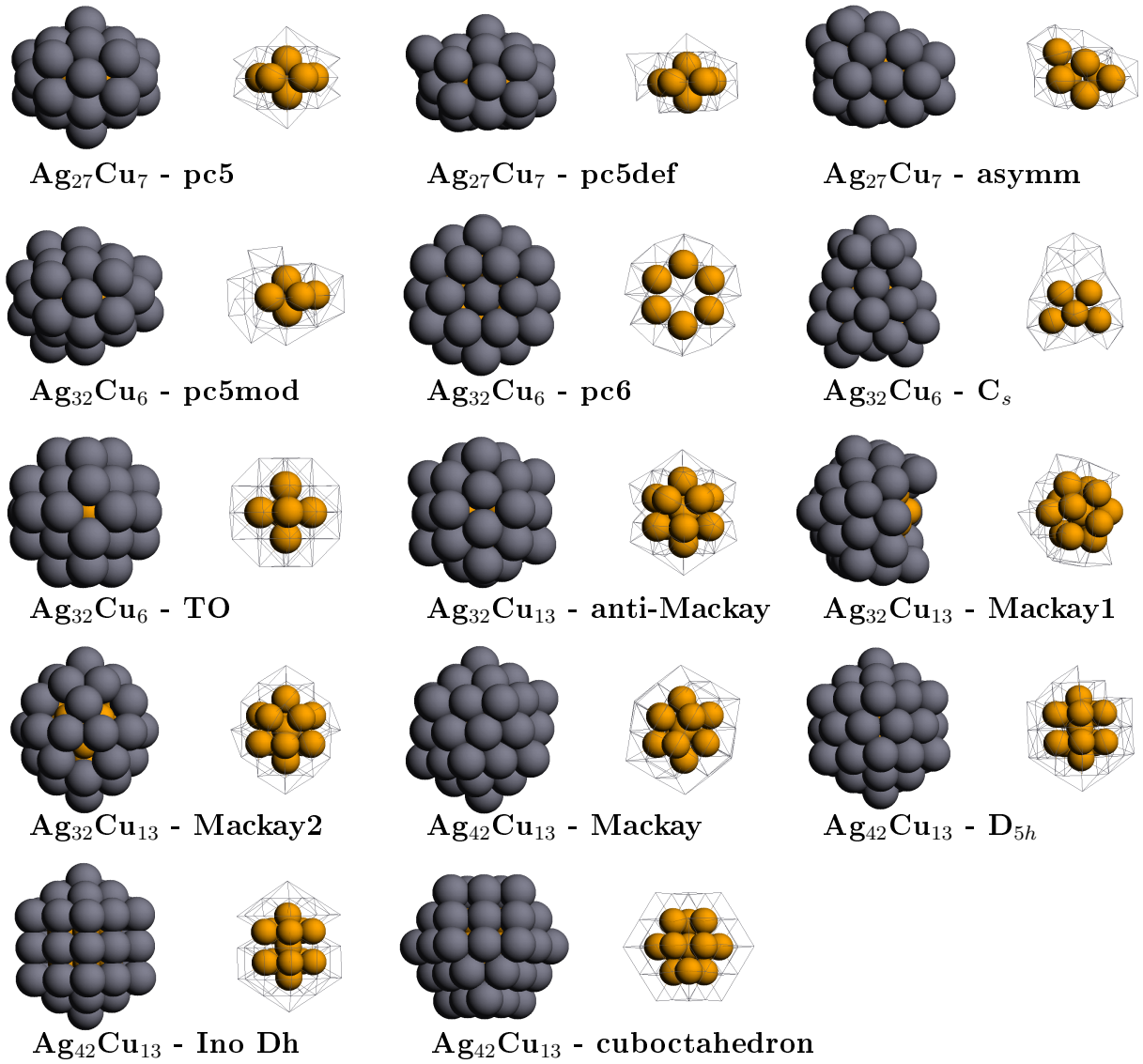

FIG. 2: Structures of large nanoalloys. Dh stands for decahedron.